

Vertical Axis Wind Turbine for Sri Lankan Southern Highway

Samidu Perera, Dilumi Nandasena, Dilini Wijayakumara and Kasuni Guruvita

Department of Electrical and Electronic Engineering,

Sri Lanka Institute of Information Technology

Malabe, Sri Lanka

{samidu72, diluminandasena, [dwijayakumara}@gmail.com](mailto:dwijayakumara@gmail.com), Kasuni.g@sliit.lk

ABSTRACT

Based on studies, most of the areas in Sri Lanka have an average amount of wind that could be resourceful in generating wind power. The area from Colombo along the coastal line to Matara is considered to have less wind potential. It's a major disadvantage to the country's energy generation plan as wind is one of the best renewable energy sources available in Sri Lanka. Concerning the energy crisis in the country, the necessity for a renewable energy source has arisen. Since renewable resources are used as standalone systems, the level of advancement increases while reducing the amount of stress on the main electrical grid when balancing the frequency. Highways can be followed as one of the country's leading divisions that could be used for the use of renewable energy. The southern expressway in Sri Lanka requires an average of 375 kW of electricity only for lighting purposes. If the lights are turned on for 12 hours, then the amount of energy requirement is 4,500 KWh. It would save a considerable amount of energy from the national grid if that energy could be provided using renewable sources. This reduction of energy consumption from the main grid would benefit both the authorities of the Sri Lankan power system and the public. To address the aforementioned issue, a vertical axis wind turbine is proposed in this project to be installed on highways. The main requirements of the project are highlighted in the introduction and problem statement. All the details of the outcomes such as optimized rotor, gear system, generator and the PIC-based power management system are explained in detail with the steps taken to optimize the system at every possible step. There are plans which may facilitate the future development of the product included in the latter part of the document.

KEYWORDS: *Highway and Wind Power, Power Systems, Renewable Energy, Vertical Axis Wind Turbine, Wind Power Generation, Wind Power Plant, Wind Turbine Model*

1 INTRODUCTION

The requirement for power has increased drastically in the previous decades in Sri Lanka. The growth factor of the power requirement is increasing while leading the country into an energy crisis. According to the power control authorities, the requirement of higher demand is fulfilled by maximizing the power generation in diesel and coal power plants. This will result in a polluted environment. The use of renewable energy sources such as wind and solar are alternative methods of generating power, which will address the energy crisis. According to experts, wind power is the most reliable and widely available renewable source of energy. Subsequently, the urban areas in Sri Lanka utilize less wind power due to the unavailability of spaces to install wind turbines. Thus, the requirement of a small-scale wind turbine arises in the domain of renewable energy. Highways in the country have a wider potential for wind coverage due to the unavailability of skyscrapers compared to coastal areas, where the available wind farms are located. One such sector of the country can be focused on developing a vertical axis wind turbine as in many other developed countries. These turbines are suitable for small wind scales and can be used to illuminate the highways during night time. Therefore, developing such a wind turbine would be a major advancement for this country.

2 LITERATURE REVIEW

2.1 Advantages of Wind Power

Sustainability of energy is closely correlated to the world's well-being and prosperity. In modern society, the need for affordable and steadfast energy sources has become a basic necessity. Hydrocarbons, such as heavy oils are the main sources of fuel for energy requirements in the world (Imperial, n.d.). The consumption of these fossil fuels has a significant effect on the atmosphere in the form of emitting toxic atmospheric pollution, causing numerous environmental problems, such as global warming and climate change (Union of Concerned Scientists, 2014). Therefore, decreasing the consumption of such non-renewable energy sources has become a major global initiative. As a result, several green energy harnessing strategies have been developed that have a much lower effect on the atmosphere relative to fossil fuels, such as wind power. Due to its benefits in the field of energy development, wind energy is one of the world's fastest-growing sources of energy. Effectively, the use of wind power also reduces hazardous waste emissions. Wind energy will therefore have the right solutions in place to address the energy crisis and its consequences (El. maksod, 2018). As the cost of wind power per kWh is much lower than that of other energy resources, wind power is remarkable for its cost-effectiveness (El. maksod, 2018). Also, the power generated by wind turbines is sold at a fixed price for a long period and rapid changes in bills are not accounted for, in these cases (Inspire, n.d.). The large space required by the wind turbines can be utilized with cultivation, making them efficient in every aspect. Referring to the factors discussed, wind energy can be identified as one of the best renewable energy sources that can be used in the Sri Lankan context.

2.2 Requirements in Generating Wind Power

In order to develop wind power in any region, a set of parameters should be considered. These must be the vital necessities that need to be identified before designing a wind turbine. One of the parameters is the availability of room for mounting wind turbines. Open spaces are generally regarded as potential locations for wind farms. Besides, prior to the development of a design, sensitive areas and other locations are also considered. For wind turbines, this is commonly referred to as the Setback (American Wind Energy Association, n.d.). The availability of suitable wind speeds in the selected area is another requirement. If the wind speeds are very low, there will be less power generation. Environmental constraints are also one of the most important considerations in wind turbine design. Despite the turbine type, either a vertical axis or a horizontal axis, some of the factors mentioned above were treated mutually in the design stage. The space requirement of a vertical axis wind turbine (VAWT) is comparatively smaller than that of a horizontal axis wind turbine (HAWT). To apply these turbines in highly dense areas, the noise level generated must be relatively low.

2.3 Highways and Wind Power

The space of the median between the lanes on the highway should be wide enough to install a VAWT. Highways consist of both natural and uncontrolled turbulent flow of the wind. The demand for designing vertical axis wind turbines remains higher compared to other wind turbines. The application area would be highways that have a sufficient amount of wind potential to run a VAWT. The designs are required to support the boundary limits between the motorways and edges. It is important to obtain accurate wind speed data for the site in mind before any decision can be made as to its suitability (ROYMECH, 2019). Wind turbines provide high power levels in open space because of their higher capacity factors. This is beneficial when the wide spaces between the motorways are not covered with obstacles.

3 METHODOLOGY

3.1 Acquisition of Wind Data in Highways

Data acquisition was conducted at the peak and off-peak hours of the day to assess the intensity of wind velocity on the highway. In deciding the average wind speed needed to operate the VAWT in a rated environment, the detection of wind patterns is important. Also, to model the turbine limits, the maximum or peak velocity was obtained. The data acquisition was performed in the outer circular expressway (E02) near the Kothalawala interchange covering the peak and off-peak time from 8.00 AM to 10.00 AM and 4.00 PM to 6.00 PM.

The device configuration for the measurement of wind data consisted of a digital anemometer, an Arduino Nano and a data recording and a storage SD card module. Once the relevant data sets were collected, the peak and average wind speeds were determined by manipulating those values. The average wind velocity was estimated as 6.3 m/s during the peak time, while the off-peak wind velocity was measured as 6.19 m/s. Those values were used for calculations and simulations in the following sections.

3.2 VAWT Rotor Design

The design process of the rotor to obtain the optimum output with regards to the project objectives was conducted under three main steps such as determination of initial turbine parameters, mathematical representation and calculations of the rotor and simulation-based modelling of the blade.

3.2.1 Determination of Initial Turbine Parameters

Estimation of initial parameters is required to be specified to provide proper guidance to the design procedure. There are several approaches to estimate these values by referring to research papers, analysing data extractions from turbines of similar markets, and using logical explanations. Rotor radius is one of the most crucial parameters that is required in the turbine design. If the rotor is too large, there is a possibility of hindering vehicle movements on the highway. Therefore, by considering factors such as the width of the median strip, an average value of 0.75m was obtained as the rotor radius. Blade length is also essential for the calculations of swept area and aspect ratio. Even though the power production increases with the blade length, the cost of implementation is also increased. Therefore, the blade length was selected to be an optimum value. After fine considerations of the installation region and the cost of design, a length of 1m was selected as the blade length value. Furthermore, the turbine height was decided to be taken as 2m (Ahmad Sedaghat, 2018). The maximum amount of wind was required to obtain the maximum power output. Hence, by using the data acquisition and analysis that were done on the highway, the wind velocity value was defined as 6.3 m/s. The tip speed ratio was taken according to research data. For Darius rotors, it has been found that the maximum efficiency of 30% to 35% can be obtained with a tip speed ratio ranging from 5-6 (Hassan, 2014/2015). Therefore, the tip speed ratio was selected as 5 for our design. The number of blades for the design was selected as three since the optimum performance can be obtained using 3 blades. Moreover, the chord length was selected as 0.2m to maintain the chord/radius ratio within the range of 0.1 to 0.4 as specified in research findings.

Additionally, the blade material was decided to be aluminium since they are durable, available as well as cost-effective. Airfoil or the blade profile is one of the crucial parameters in designing the turbine blade. A set of steps was followed to adapt the best existing airfoil for our project. First, the Reynolds number for the design was roughly calculated. Then by analysing the research papers for similar designs, the most suitable types of airfoils were selected. Accordingly, traditional small vertical axis wind turbine airfoils such as NACA 0015, NACA 0018, and NACA 0021 were compared to select the optimum choice. A thicker airfoil design was needed to be selected for efficiency at low wind speeds. Therefore, NACA 0021 was selected as the airfoil for our design (Airfoil Tools, n.d.).

The initial angle of attack (α) was selected as 0° because higher values of the angle of attack are only beneficial for higher values of tip speed ratios. The pitch angle (β) was also selected as 0° because it was decided to have a fixed pitch (stall control) in the design.

3.2.2 Mathematical Representation and Calculations of the Rotor

The subsequent step in the design process of the rotor is the mathematical representation of the rotor parameters. Calculations of swept area, wind power, power coefficient, mechanical power, angular speed, mechanical torque, the Reynolds number, solidity and aspect ratio are required for this procedure.

Swept area is known as the region of air that encompasses the turbine in its rotation. The swept area of an H-rotor VAWT takes a rectangular shape (El. maksod, 2018). It was calculated using the following equation where S is the swept area (m²), R is the rotor radius (m), and L is the length of the blade (m).

$$S = 2 \times R \times L \quad (1)$$

The power harvested from the wind (P_W) is an important parameter to determine the performance of the turbine. It was calculated using the following equation where ρ is the air density (1.225 kg/m³), V_0 is the velocity of the wind (m/s), and S is the swept area (m²).

$$P_W = \frac{1}{2} \times \rho \times S \times (V_0)^3 \quad (2)$$

Power coefficient (C_P) is used to calculate the captured mechanical power by the blades. It can be also derived from the efficiency of the wind turbine. Based on the tip speed ratio and pitch angle, the following equation was adapted to calculate the C_P value.

$$C_P(\lambda, \beta) = C_1(C_2\lambda_1 - C_3\beta - C_4)E^{\frac{-C_5}{\lambda_1}} + C_6\lambda \quad (3)$$

Where, $C_1=0.5176$, $C_2=116$, $C_3=0.4$, $C_4=5$, $C_5=21$ and $C_6=0.0068$ are constant coefficients. λ is the tip speed ratio and β is the pitch angle. λ_1 is defined as follows.

$$\frac{1}{\lambda} = \frac{1}{\lambda + 0.08\beta} - \frac{0.035}{\beta^3 + 1} \quad (4)$$

The mechanical power (P_m) was derived in Watts using the available wind power and power coefficient as given below.

$$P_m = \frac{1}{2} \times \rho \times S \times (V_0)^3 \times C_P(\lambda, \beta) \quad (5)$$

The angular speed (ω) was calculated in rad/s using the equation defined for the tip speed ratio is given below.

$$TSR(\lambda) = \frac{R \times \omega}{V_0} \quad (6)$$

The mechanical torque (T_m) was calculated in Nm using the captured mechanical power by the blades and the angular speed of the rotor as follows.

$$T_m = \frac{P_m}{\omega} \quad (7)$$

The Reynolds number is a significant parameter that is used in selecting the proper airfoil design for the turbine. Better performance can be achieved with a higher Reynolds number. This is because when the Reynolds number increases, the lift coefficient increases while decreasing the drag coefficient (S. Brusca, 2014). Hence, the Reynolds number was calculated by adapting the following equation where, V_0 is the free-stream wind speed (m/s), $\lambda_{CP(max)}$ is the tip speed ratio that maximizes C_P , c is the chord length (m), and ν is the kinematic viscosity of the fluid (m²/s).

$$Re = \frac{V_O \times \lambda_{CP(\max)} \times c}{v} \quad (8)$$

The solidity of the turbine is known as the total cross-sectional area of the side of the blades to the frontal swept area. If the solidity is higher, the self-starting torque is increased. Therefore, the drag component is increased. Hence, solidity must be kept at a lower value to get the turbine to start rotating (Ibrahim Ara). The solidity (σ) was calculated using the equation given below where, N is the number of blades, c is the blade chord (m), and R is the rotor radius (m).

$$\sigma = \frac{N \times c}{R} \quad (9)$$

Aspect ratio (AR) is defined as the ratio between the blade height and the rotor radius. To maximize the power coefficient value, the rotor's aspect ratio must be kept as small as possible. Hence, the turbine performance can be derived using this parameter (S. Brusca, 2014). The following equation was used to calculate the aspect ratio.

$$Aspect\ Ratio\ (AR) = \frac{Height\ of\ the\ blade\ (length)}{Rotor\ radius} \quad (10)$$

3.2.3 Simulation-Based Modelling of the Blade

Simulation-based modelling was performed as the next step of the design process to obtain verification of the turbine performance. For this purpose, it was decided to use programs such as MATLAB Simulink and QBlade because of their reliability, simplicity, and less consumption of time. MATLAB was used to develop the mathematical model of the design while QBlade software was used to simulate the rotor blade and obtain graphical interpretations of the blades.

3.3 Gear System and Generator Design

Based on literature and background analysis, the design process of the generator and the gear system to obtain the optimum output with regards to the project objectives was conducted by mathematical representation and calculation of the gear system and generator, simulation-based modelling of the gear system and the generator. A set of equations and mathematical parameters were used in determining the parameters. Once the calculations were performed, those outcomes were verified using the simulation models while differentiating errors.

3.3.1 Mathematical Representation of the Gear System and the Generator

Based on literature and background analysis, a set of equations and mathematical parameters were used in determining the generator and gear parameters. The following section describes out the continuation of the design based on mathematical equations.

According to the breakdown of gear systems, a spur gearbox with a lower gear ratio was selected for the design considering the reliability, simplicity, low cost of building and designing, non-complex gear analysis and easy simulations. Before continuing the design details and calculations, a set of parameters and equations were referred to identify the vital design procedures and techniques in gearing.

Gear tooth systems known as the diametral pitch system and the module system, specify the connection between addendum, dedendum, working depth, tooth thickness and pressure angle. In the gear system, increasing the gear module results in larger teeth designs, while increasing the pressure angle results in smaller teeth designs. These elements and theories were studied in calculating gear system parameters during the designing phase. The gear efficiency and the torque conversion are some of the vital aspects in determining the gear type. The efficiency of the gear system was calculated using the equation mentioned below.

$$\eta = \frac{Output\ shaft\ power}{Input\ shaft\ power} \times 100\% \quad (11)$$

Power losses were mainly concerned with tooth friction and lubrication losses in the gear systems. According to studies, the losses were mostly related to the peripheral velocity of the fluid rotating through the gears. Frictional losses in the gears are related to the configuration of the gear, the reduction ratio, the angle of pressure, the height of the gear and the friction coefficient (Bin Wu, 2011). Since losses are hard to quantify, during the initial gear design, calculations based on practices were often used.

The following remarks were mostly referred to estimate the percentage of the gear train efficiency correlated with tooth friction. A basic table is given below showing the efficiencies of various types of gears. The efficiencies for each mesh in the line are multiplied together to calculate the efficiency for the entire drive train.

Table 1 Gear efficiencies related to different gear types (Bin Wu, 2011)

Type	Gear Ratio	Efficiency
Spur	1:1 to 6:1	98-99%
Helical	1:1 to 10:1	98-99%
Double Helical	1:1 to 15:1	98-99%
Bevel	1:1 to 4:1	98-99%
Worm	5:1 to 75:1	20-98%
Crossed Helical	1:1 to 6:1	70-98%

When designing the gear system, a proper efficiency calculation along with the percentage power loss was carried out without using the approximated gear efficiencies. Particularly, a spur gear was selected considering the ease of calculations and efficiency. Hence, a gear ratio of 4:1 was selected. Since the design is a single mesh gear system having a pinion gear and a spur gear, the following mathematical equations were used to calculate the percentage power loss (P). where R_g is the Gear ratio, R_o is the Gear outside diameter (m), r_o is the Pinion outside diameter (m), d_G is the Gear pitch diameter (m), d_P is the Pinion pitch diameter (m), α is the Pressure angle and μ is the Friction coefficient.

$$P = \frac{50\mu}{\cos\alpha} \left[\frac{H_S^2 + H_t^2}{H_S + H_t} \right] \quad (12)$$

$$H_S = (R_g + g) \left[\sqrt{\left(\left(\frac{R_o}{d_G} \right)^2 - \cos^2 \alpha \right)} - \sin \alpha \right] \quad (13)$$

$$H_t = \left(\frac{R_g + g}{R_g} \right) \left[\sqrt{\left(\left(\frac{R_o}{d_G} \right)^2 - \cos^2 \alpha \right)} - \sin \alpha \right] \quad (14)$$

The generated torque from the turbine was transferred into the generator by using a gear train. When using a pinion gear system connected to the main gear, the torque can be either higher or lower than the torque of the gear connected to the turbine. It is proportional to the gear ratio and inversely proportional to the angular speed of the gears, which was calculated using the following expression where ω_P is the Angular velocity of the pinion, ω_G is the Angular velocity of the gear, d_P is the Diameter of the pinion, d_G is the Diameter of the gear, T_P is the Torque of the pinion and T_G is the Torque of the gear.

$$\frac{\omega_G}{\omega_P} = \frac{d_P}{d_G} = \frac{N_P}{N_G} = \frac{T_P}{T_G} \quad (15)$$

Therefore, the torque delivered to the generator was calculated from the following expression, where T_G is equal to the mechanical power delivered from the wind turbine.

$$T_P = T_G \times \frac{N_P}{N_G} \quad (16)$$

A permanent magnet synchronous generator was selected as the generator for the vertical axis wind turbine considering the factors discussed in previous sections. PMSG has a different set of configurations and power control techniques, which were considered during the design phase. However, some were highly cost-effective when it came to the selection of permanent magnets. Therefore, a simpler and more accurate mathematical model was used in the design stage of the generator.

The mathematical model of the generator was formulated using a set of equations required to calculate the generator parameters. According to (Y. Erramia, 2013), the following set of equations was used. First, the electromagnetic torque generated in the system was found. Using the expression given below. Where, L_d , L_q is the d and q axis self-inductance, P is the number of pole pairs and λ_r is the rotor flux linkage.

$$T_e = \frac{3P}{2} (\lambda_r i_{qs} - (L_d - L_q) i_{ds}) \quad (17)$$

i_{qs} and i_{ds} are dq axis current components, which were found using the following two equations. Where, R_s is the resistance of the stator winding and v_{ds} and v_{qs} are the voltages of the dq axis in the stator.

$$\frac{di_{ds}}{dt} = -\frac{R_s}{L_d} i_{ds} + \frac{L_q}{L_d} \omega i_{qs} - \frac{1}{L_d} v_{ds} \quad (18)$$

$$v_{ds} = -R_s i_{ds} + \omega_e L_q i_{qs} - L_d \frac{di_{ds}}{dt} \quad (19)$$

The voltages of the stator windings were found using the following equation, concerning the generator electrical speed (ω_e), stator inductance, stator resistance and dq axis currents.

$$v_{ds} = -R_s i_{ds} + \omega_e L_q i_{qs} - L_d \frac{di_{ds}}{dt} \quad (20)$$

$$v_{qs} = -R_s i_{ds} - \omega_e L_q i_{qs} + \omega_e \lambda_r - L_d \frac{di_{ds}}{dt} \quad (21)$$

ω_e in the equations given above are known as the electrical angular speed of the generator, which was calculated using the following formula.

$$\omega_e = \omega_g \times P \quad (22)$$

Most of the synchronous generator types consist of different power control strategies. These are used to significantly increase the amount of power generated. Among the control strategies of maximum power point tracking, pitch control, excitation current vector control and grid side control strategies, vector control provides a more efficient conversion of energy during variable wind speeds (Hassan, 2014/2015). Thus, this technique was used in determining the power and torque.

Excitation of the current vector control of the generator provides better control over the linear relationship between the stator current and the electromagnetic torque while delivering the maximum torque with a minimum stator current (Rim Ben Ali, 2017). Therefore, when calculating the generator parameters, i_{ds} was kept at zero. In that case, the electromagnetic torque and the stator currents were calculated using the following expressions.

$$T_e = \frac{3P}{2} \lambda_r i_{qs} = \frac{3P}{2} \lambda_r i_s \quad (23)$$

$$i_s = \sqrt{i_{ds}^2 + i_{qs}^2} = i_{qs} \quad (24)$$

Then the mechanical power at the generator shaft was calculated using the equation given below, acknowledging T_g and ω_g as the torque and the rotational speed of the gear system.

$$P_m = T_g \omega_g \quad (25)$$

The active power (P_L) delivered to the system was less than the mechanical power because of the stator copper losses ($P_{cu,s}$). Thus, the stator copper loss was calculated as follows.

$$P_{cu,s} = 3I_s^2 R_s = 3I_s V_s \quad (26)$$

$$P_L = P_m - P_{cu,s} \quad (27)$$

Since i_{ds} was considered as zero, the stator current and voltage were found using the following equations. Also, the 3-phase voltage and current values of the generator were calculated once the following parameters were obtained.

$$I_s = \frac{i_{qs}}{\sqrt{2}} \quad (28)$$

$$V_s = \frac{v_{qs}}{\sqrt{2}} \quad (29)$$

3.3.2 Simulation of the Gear System and the Generator

The gear system parameters were assumed based on the background analysis when using the mathematical equations for gear design. For the MATLAB simulation, some of the assumed parameters such as the gearing ratio and the centre distance between the gears were moderated depending on the standards from gear manufacturers. Then the SIMULINK software was used to determine the number of teeth in the spur gear and pinion gear.

Thereafter, determination of the torque was generated, and power conversion efficiency was performed using the results obtained by the previous simulation. The simulation required a set of other parameters such as pressure angle, pitch diameters and the friction coefficient. These are preferred to retain the requirements as the mentioned in the literature review. Eventually, another simulation block was used to connect the turbine and the generator simulation blocks.

When specifying parameters for the generator simulations, some of the parameters were determined using the available designs as mentioned in the previous section. When the simulations were performed, some of the software programs delivered opposing results. Therefore, the existing generator parameters were compared when validating the simulations. The main objective of the simulation was to test the proposed generator's performance under various conditions. MATLAB Simulink outperformed most of the power analysis software packages. Thus, it was used for the evaluation of the generator. The torque transferred from the gear model was transmitted into the PMSG subsystem to generate the power, based on the given stator parameters and machine characteristics. Then the generated alternating voltage and current components were measured using the V-I measurement block. These values were compared with the existing power quantities. A load was added to represent the direct use of dc voltage and the current components deduced from the Universal Bridge, which consists of six power diodes. The representation of the generator system can be given in the following simulation model.

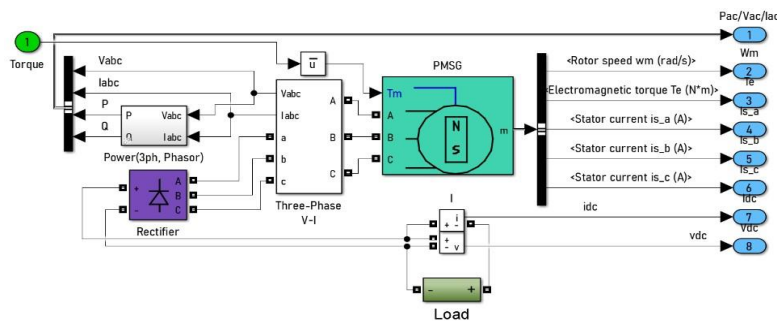


Figure 1 Simulink block diagram of a modelled PMSG system

However, controlling the fluctuation of frequency and the output voltage relevant to a variable wind speed was not accounted for in this model. Therefore, the generated voltage and the frequency were fluctuating according to the average wind speed. The machine was modelled using a dual-phase magnetic flux frame with equal d and q axis inductance and phase-shifted by 90 degrees. This was implemented in the system by the PMSG system block diagram in the above model. Once the simulation was performed, the output scopes displayed the amount of active and reactive power, electromagnetic torque, and dc quantities of the model.

3.4 Charge Controller Design

The wind charge controller of the system is designed and simulated using the Proteus software. The micro-controller PIC12F675 is used as the controlling component of the circuit as it is cost effective and more reliable for small scale applications.

3.4.1 Battery

Lead-acid batteries are deep-cycle batteries, which are ideal for small-cycle renewable energy integration applications. Due to their construction, it is suitable for small scale wind energy projects and requires low maintenance. They are widely used in off-grid power systems and similar roles. The voltage of the selected battery was in the range of 12 Volts and the current was in the range of 20Ah.

3.4.2 Charge Controller

The voltage generated by the wind turbine was considered as 200VAC. Thereafter that voltage was stepped down for about 20VAC. After that, the voltage was regulated to 13.8 VDC. The charging and discharging of the battery are controlled by a PIC12F675 micro-controller as it can read a range of analog signals, unlike PIC16f877A which can only read a referenced analog signal (MICROCHIP, n.d.). During the design stage, the 12V output of the battery was stepped up to 220V before passing the voltage to the load. The load was a 250/220V High-Pressure Sodium (HPS) bulb.

3.4.3 Circuit Implementation

There was no similar component to a wind turbine in the Proteus software. Therefore, an AC voltage source was used as the input to the circuit. The source had a constant current of 20A. The voltage regulator LM7805 was used to feed the 5V to the micro-controller. The voltage received from the turbine was regulated to 13V by a Zener diode and then it was sent to the battery by using the PWM technique to charge the battery (EL-PRO-CUS, 2013). The PIC12F675 was used to control overcharging, discharging, and cut-off of the battery. There is an inbuilt oscillator in this micro-controller which was used to obtain a periodic signal to control the voltage. In this micro-controller, a soft PWM was used to activate the PWM module. When the battery was charged using the PWM technique, an LED was used to detect whether the battery was charging. When the battery was fully charged, PWM emitted a small pulse with less pulse width into the battery to eliminate charging the battery.

Furthermore, the drain cut-off was done using a 5V relay. When the battery was charging the relay was in the normally open position and when the battery was discharging up to about 11V, the relay was shifted to the normally closed position. Then the LED indicator was turned off. As the relay was a 5V relay, the battery voltage could be used to function it. The 555 timers were used to generate and divide pulses in the inverter circuit (Electronic-Tutorials, n.d.). Then the 12VAC was obtained and it was stepped up to 240VAC by using a centre-tapped transformer with a 1:20 winding ratio (COMPONENTS101, 2018). After that, this voltage was sent to the load, which was a 230V,250W HPS bulb. The voltage of 240VAC was obtained to compensate for the losses in the circuit. The image given below shows the arrangement of the components in the circuit.

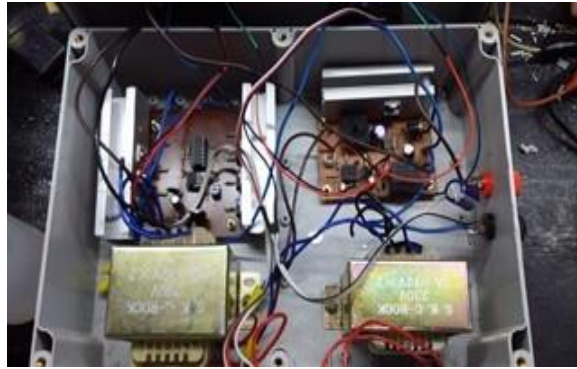


Figure 2 Charge Controller

4 DISCUSSION

The amount of power that can be efficiently generated from a particular turbine depends on the area enclosed by the rotor blade. According to this theory, the designing of VAWT for Sri Lankan highways was carried out followed by a data analysis. This provided a clear overview of the amount of power that can be generated. The analysis of wind speeds obtained from a digital anemometer concluded the average wind velocity as 6.3 ms^{-1} .

The turbine rotor design was performed with the aid of manual calculations as well as simulation-based modelling using QBlade and MATLAB Simulink software programs. The results obtained using the QBlade software includes airfoil design, rotor blade design, rotor DMS simulation, multiparameter DMS simulation, turbine DMS simulation, and turbulent Windfield generation. Given below is a representation of the simulation.

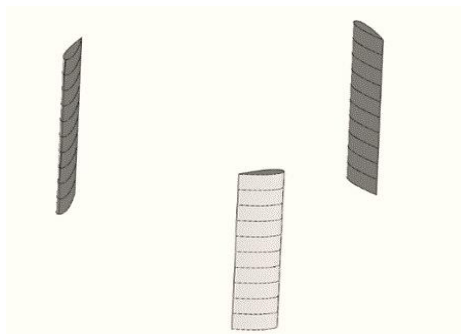


Figure 3 Rotor blade design

When comparing the results of manual calculations and simulation-based modelling, some slight deviations in wind power, power coefficient, mechanical power, rotational speed, and mechanical torque were observed. The main reason for this difference in values is the computational changes when calculating the power coefficient. A slight change in constants used in the manual calculation and simulation can cause a significant difference in the outcome. Nevertheless, the deviation can be overlooked as because the range of error is considerably low. The table given below illustrates the comparison between the results and the parameters used.

Table 2 Comparison between the results and parameters

Parameters	Calculation	Simulation
Rotor radius	0.75 m	0.75 m
Blade length	1 m	1 m
Turbine height	2 m	2 m
Wind velocity	6.3 m/s	6.5 m/s
Tip speed ratio	5	5
Number of blades	3	3
Airfoil	NACA 0021	NACA 0021
Blade chord	0.2 m	0.2 m
Angle of attack	0°	0° and 9.5°
Pitch angle	0°	0°
Swept area	1.5 m ²	1.5 m ²
Power in wind	229.73 W	252.31 W
Power coefficient	0.2628	0.354
Mechanical power	60.373 W	93.89 W
Rotational speed	401.07 rpm	400 rpm
Mechanical torque	1.437 Nm	2.24 Nm

It is beneficial to comprehend how particular changes in parameters can influence turbine efficiency. One such parameter which directly affects the turbine performance is the tip speed ratio. When observing the relationship between TSR and power coefficient, initially the power coefficient increased with the TSR, after reaching a threshold value, the power coefficient gradually decreased. Hence, to maximize the performance of the turbine, an optimum value of TSR must be selected. Furthermore, it was noticed that higher power outputs can be gained with higher wind velocities. But the output of the turbine is at its highest when the torque entering the generator corresponds to the angular velocity of the turbine. Moreover, it is clear that by increasing the blade chord, rotor radius and blade length, the rotor performance increases as well.

The calculation carried out for the gear train design was used to determine the feasibility of using the gear train design on the vertical axis wind turbine project. When considering the results of the gear system, the torque and the velocity of the connected gears were clarified. In the gear design, the pinion and the main gear were designed to prevent losses due to friction. Thereafter, a set of new gear diameters and tooth sizes were selected because the mathematically modelled gears had a larger diameter compared to the overall design dimensions and the power loss was relatively higher. The pitch angle of the simulation was changed to 25° based on the performance. Once the space between the gears was selected, it was utilized to find the diameters of the gear and the pinion. Pitch diameter was also altered depending on the losses in the system.

The output AC power, current and voltage from the generator were compared with the variation of generator models. Parameters such as stator resistance, dq axis inductance, flux linkage and the number of poles

were changed accordingly to obtain the most reliable outcomes using the simulation. The purpose of the simulation was to validate the variation between the electrical power and the attributes of the generator.

The amount of peak power from the model was simulated as 42W at 90VAC. Since the available wind velocity average was 6.3ms^{-1} , the amount of power generated was also reduced. The design was capable of providing an annual power rating of 0.368 MWh, which is a sizable amount of power compared to non-renewable energy sources. The amount of DC power generated was measured using a load connected at the generator terminal. The load was rated with a value of 150 ohms. The peak value of the DC voltage was around 93V while the peak current was at 0.55A.

In the charge controlling system, the PIC12F675 microcontroller is the controlling element of the system. The main application of the algorithm built into the PIC12F675 microcontroller is designed and optimized to perform the charging and discharging of the battery and to control relay on/off control for drain cut-off. Further, when creating the code, the upper limit of the battery is assumed as 13V, and the lower limit is assumed as 11V. The algorithm does not allow the draining of the battery voltage below the lower limit, and it performs fast-charging up to 70% of the battery capacity (GLOBAL-CIRCUIT, n.d.). After that, it sends PWM pulses with a delay which is about 5 seconds when the battery is charging from 70% to 100%. This is done to reduce the rate of charging. To indicate the charging of the battery, a blinking green LED bulb is used.

The completed project consisted of other system models that performed well in the simulations and the variation of wind power affected the overall efficiency of the system. Higher wind velocities were capable of producing higher electrical power. But the simulated model had its limitations in many cases, which affected the overall performance of the wind turbine.

5 CONCLUSION

An H-rotor Darrieus turbine was selected as the rotor type for this application considering its simplicity and cost-effectiveness. Initially, 6.3 m/s was derived as the average wind speed from the data analysis. Next, focusing on the available low wind speeds a thicker airfoil design (NACA 0021) was selected as the blade profile. Furthermore, a rotor radius of 0.75 m, blade length of 1 m, turbine height of 2 m, blade chord of 0.2 m and a tip speed ratio of 5 were selected as parameters in the design procedure. To model the performance of the turbine, two simulation software programs were used. Accordingly, the mechanical power was estimated as 60.373 W with a mechanical torque of 1.437 Nm.

The amount of turbulent wind was inadequate to produce a constant rotation in the generator. Therefore, a linear gear system was included in the design. A PMSG was used in the wind turbine model to eliminate the use of electricity to excite the generator, making the design more renewable. Based on the determined wind data, the turbine height was selected as 2m. The average wind speed of 6.3ms^{-1} produced an electrical power of 42 W continuously in the simulation, using a rotor blade consisting of a height of 1m and a radius of 0.75 m. This amount of power is sufficient for small applications such as lighting.

The charge controller system was focused to manage and optimize the power harvested from the wind. Besides that, the charge controller has successfully managed the battery discharging and charging processes during the peak and off-peak periods of wind sources. The generated voltage of 220VAC was stepped-down to 20VAC and was regulated to 13VDC. Then the regulated voltage was used to charge the 12V battery and to power the load when necessary. The charge controller system increased the utilization of the available energy sources or stored energy with the least dependency on the grid network for the power source supply.

REFERENCES

- Ahmad Sedaghat, E. B. (2018). Feasibility of highway energy harvesting using a vertical axis wind turbine. *Energy Engineering: Journal of the Association of Energy Engineers*.
- Airfoil Tools*. (n.d.). Retrieved 10 01, 2020, from <http://airfoiltools.com/airfoil/details?airfoil=naca0021-il>
- American Wind Energy Association*. (n.d.). Retrieved 10 28, 2020, from <https://www.awea.org>
- Bin Wu, Y. L. (2011). *Power Conversion and Control of Wind Energy Systems*. Wiley-IEEE Press.
- COMPONENTS101*. (2018). Retrieved 2020, from <https://components101.com/transformers/12-0-12-center-tapped-transformer>
- El. maksod, I. G. (2018). *Performance Analysis - Design and Manufacturing of Vertical Axis Wind Turbine*.

- Electronic-Tutorials.* (n.d.). Retrieved 2020, from https://www.electronicstutorials.ws/waveforms/555_timer.html
- EL-PRO-CUS. (2013). Retrieved 2020, from <https://www.elprocus.com/full-wave-bridge-rectifier-versus-center-tapped-full-wave-rectifier/>
- GLOBAL-CIRCUIT.* (n.d.). Retrieved 2020, from <https://circuitglobe.com/lead-acid-battery.html>
- Hassan, A. (2014/2015). *Based Design and Development of a Vertical Axis Wind Turbine Computational Model.* Leicester.
- Ibrahim Ara, F. A. (n.d.). Highway Vertical Axis Wind Turbine with Vortex Generators.
- Imperial.* (n.d.). Retrieved 10 27, 2020, from <https://www.imperialoil.ca/en-CA/Company/About/The-importance-of-energy>
- Inspire.* (n.d.). Retrieved 10 27, 2020, from <https://www.inspirecleanenergy.com/blog/clean-energy-101/advantages-of-wind-energy>
- MICROCHIP. (n.d.). (MICROCHIP) Retrieved 2020, from <https://www.microchip.com/wwwproducts/en/PIC12F675>
- Rim Ben Ali, H. S. (2017). *Modeling and Simulation of a small Wind Turbine system based on PMSG generator.* Slovenia.
- ROYMECH.* (2019). Retrieved 10 10, 2020, from https://roymech.co/Useful_Tables/Drive/Gear_Efficiency.html
- S. Brusca, R. L. (2014). Design of a vertical-axis wind turbine and how the aspect ratio affects the turbine's performance.
- Union of Concerned Scientists.* (2014, 06 19). Retrieved 10 27, 2020, from <https://ucsusa.org/resources/environmental-impacts-natural-gas>
- Y. Erramia, M. O. (2013). Control of a PMSG based wind energy generation system for power maximization and grid fault conditions. *Mediterranean Green Energy Forum MGEF-13*(42), 220-229.